This study considers analog high-frequency (HF) communication systems that use broadband signals modulated by the Barker code. The task addressed is to improve the efficiency of analog HF communication systems when transmitting broadband signals.

Patterns in the formation of a noise-resistant broadband signal with phase modulation by the Barker code and the operation of the signal spectrum expansion and restoration unit have been investigated. It was established that phase modulation makes it possible to achieve such a spectral width, amplitude of the main peak of the autocorrelation function, and time resolution, which enable effective correlation separation of the usable signal and increases its noise immunity.

It has been shown that signal modulation with a five-bit code forms a spectrum with a width of 1 MHz, the amplitude of the main peak of the autocorrelation function is 9 units, and a time resolution of 1–2 μs, which provides an increase in noise immunity to 9 dB at S/N =1 dB compared to the base signal without modulation. The use of a thirteen-bit code allows this indicator to be increased to 13 dB at S/N = –3 dB.

The effectiveness of the module for expanding and restoring the spectrum of the modulated signal when transmitting it over a distance without loss of communication quality has been confirmed. Signal modulation with a 5- and 13-bit code, compared to unmodulated, increased the communication range by 9 and 25 times, respectively. The results are attributed to the optimal autocorrelation properties of Barker codes and hardware solutions that form a broadband signal without complicating the circuit. This is explained by the ability of Barker codes to form a narrow correlation pulse and expand the signal spectrum, which reduces sensitivity to narrowband interference.

The results are valuable for applications in analog RF communication systems as well as power grids, in particular at low S/N ratios

Keywords: autocorrelation function, analog signal, Barker code, matched filter, phase modulation

UDC 621.396.6:621.391.8
DOI: 10.15587/1729-4061.2025.340994

DETERMINING THE EFFECT OF PHASE MODULATION AND OPTIMAL SIGNAL PROCESSING ON HF COMMUNICATION SYSTEM RELIABILITY AND RANGE

Yurii Honcharenko
PhD, Associate Professor*
Gennadii Golub
Doctor of Technical Sciences, Professor**
Department of Mechanical, Energy and Biotechnology Engineering
Agriculture Academy
Vytautas Magnus University
Studentų str., 11, Kaunas, Lithuania, LT-53362
Nataliya Tsyvenkova
Corresponding author
PhD, Associate Professor**
E-mail: nataliyatsyvenkova@gmail.com
Ivan Poleshchuk
Senior Lecturer*
Anatolii Denysiuk
PhD, Associate Professor*
Ivan Omarov
PhD Student
Department of Renewable Organic Energy
Institute of Renewable Energy
National Academy of Sciences of Ukraine
Hnata Khotkevycha str., 20-a, Kyiv, Ukraine, 02049
Olena Sukmaniuk
PhD, Associate Professor*
*Department of Electrification, Production Automation and Engineering Ecology
Polissia National University
Stary blvd., 7, Zhytomyr, Ukraine, 10008
**Department of Technical Service and Engineering Management named after M. P. Momotenko
National University of Life and Environmental Sciences of Ukraine
Heroyiv Oborony str., 15, Kyiv, Ukraine, 03041

Received 16.07.2025
Received in revised form 22.09.2025
Accepted date 29.09.2025
Published date 28.10.2025

How to Cite: *Honcharenko, Y., Golub, G., Tsyvenkova, N., Poleshchuk, I., Denysiuk, A., Omarov, I., Sukmaniuk, O. (2025). Determining the effect of phase modulation and optimal signal processing on hf communication system reliability and range. Eastern-European Journal of Enterprise Technologies, 5 (9 (137)), 64–81. https://doi.org/10.15587/1729-4061.2025.340994*

1. Introduction

Over the past decades, the transmission of information signals over power transmission lines (PTLs) has been the subject of study within a large body of applied and fundamental research. This technology was first implemented in the 1910s in the USA for the transmission of analog signals and, since the 1930s, it has been used for telephone messages. Currently, there are two main types of information transmission over power transmission lines: point-to-point transmission over high-voltage power transmission lines and broadband exchange of information signals in medium and low-voltage networks (0.4...35 kV) [1].

The attractiveness of HF communication technology is explained by the possibility of using the existing infrastructure of power networks to transmit information signals

without the need for additional channels. This provides significant cost-effectiveness and independence of energy supply companies from external providers, which is critically important in emergencies [2]. At the same time, the operation of such systems occurs under conditions of increased interference, limited frequency resources, and significant energy losses over long distances, which poses new scientific and engineering challenges.

Digital modulation methods are actively being introduced in modern networks, which make it possible to significantly increase the density of transmitted information from 0.3 to 8 bit/s Hz compared to classical analog approaches. This provides a bandwidth of up to 64 kbit/s at an 8 kHz bandwidth in each direction [3]. However, such solutions require complex hardware implementation and significant computing resources, which limits their use in energy and industrial networks. Therefore, even with the active development of digital technologies, there is a need to improve analog HF communication systems capable of enabling stable data exchange at a low S/N ratio.

Classical narrowband modulation methods demonstrate satisfactory results only in the absence of intense interference. In the case of atmospheric or industrial interference, their efficiency decreases sharply. One of the promising directions for the development of analog HF communication systems is the use of broadband signals using codes with high correlation properties, in particular Barker codes. Due to the formation of an autocorrelation function with a pronounced main peak and a low level of side lobes, they provide high accuracy of signal detection against a background of noise, reduce intersymbol interference, and increase noise immunity [4].

Despite the significant potential of the indicated approach, a number of unsolved scientific problems remain. First, the complexity of the environment of electrical networks with strong electromagnetic interference, variable loads, and line heterogeneity significantly complicates the accurate modeling of transmission processes. Second, the hardware implementation of spectral spread methods needs to be improved: optimization of phase modulation using Barker codes, modernization of matched filters, development of compact analog adders and energy-efficient circuits [5]. This makes it possible to reduce hardware costs and at the same time maintain high noise immunity.

From a practical point of view, the results of these studies contribute to increasing the reliability of conventional power supply systems in which HF communication is used for network monitoring and control, as well as in critical, military, and special infrastructure. Here, the key is the ability of the system to function stably under conditions of low S/N ratio and significant interference [6].

Therefore, research aimed at devising highly efficient spectral spread methods and hardware for transmitting broadband signals in analog HF communication systems is relevant.

2. Literature review and problem statement

A promising method for increasing the S/N ratio using the temporal redundancy of information transmission is signal modulation using Barker codes [4, 5]. The theoretical foundations of this approach are laid in [7], in which the unique autocorrelation properties of Barker sequences are proven and it is established that true odd-length codes exist only for $N = 3, 5, 7, 9, 11, 13$. This result is of great importance for theory but limits the possibilities of practical use of codes in systems that require longer sequences to ensure the required signal-to-noise ratio using the temporal redundancy of information transmission. The problem of finding approaches to constructing codes that can adapt to the conditions of analog transmission channels remains unsolved, which is explained mainly by the theoretical nature of the cited study.

Further development of the idea of increasing the efficiency of Barker codes was reflected in [8, 9], in which the formation of composite codes by combining short sequences was proposed. This allowed the authors to obtain improved autocorrelation properties and reduce the level of intersymbol interference when used in phase modulation. In particular, in [8] an approach to constructing composite codes for synchronization tasks was devised, and in [9] it was proven that their use in broadband communication systems increases the reliability of reception. However, the practical implementation of such solutions in analog channels remained open since the authors limited themselves to simulation, without taking into account nonlinear distortions characteristic of real HF paths.

A more comprehensive approach was implemented in study [10], in which a comparison of composite Barker codes of length 49, 77a, and 77b with Gold codes and Kasami sequences of length 63 for broadband signal synchronization systems was carried out. The simulation results showed that the use of composite Barker codes makes it possible to increase the S/N ratio in the channel compared to other codes. Composite Barker codes of length 49 have a higher noise immunity by 1.6–22.1% compared to Gold codes and by 0.35–12.6% compared to Kasami sequences at S/N ratios from 1 to 30 dB. Only at low S/N ratios (about 0 dB) did Kasami sequences turn out to be slightly more effective, which is explained by the specific properties of autocorrelation functions in low-quality channels. The results confirm that composite Barker codes are a promising tool for increasing the S/N ratio in broadband communication systems, providing more reliable signal synchronization and reducing the impact of noise and intersymbol interference. At the same time, for practical application, it is necessary to take into account the real conditions of HF channels, in particular phase distortions, impulse noise, and nonlinear effects.

In parallel, study [11] focused on the generation and digital correlation of Barker codes. It was shown that short sequences provide high accuracy in determining the moment of signal arrival and improve autocorrelation properties in digital systems. However, as in previous works, the issue of adapting this approach to analog systems remained unresolved. The main reason is the objective technical difficulties associated with the hardware implementation of analog correlators, which are much more complex to implement compared to digital ones.

In [12], an algorithm for the synthesis of Barker codes with a low level of side peaks of the autocorrelation function is proposed, which is critical for increasing the noise immunity of signals in radio engineering systems. The mathematical model built makes it possible to generate codes with improved correlation properties, which enables more reliable signal transmission under difficult conditions. The proposed synthesis algorithm optimizes the autocorrelation characteristics of codes, which makes it promising for use in modern high-frequency communication systems. At the

same time, the study was performed by modeling in a simplified environment, without checking the efficiency of codes in real channels with phase distortions, impulse noise, and nonlinear effects. Further implementation of the algorithm in practical systems requires taking into account these physical parameters of the environment and adapting the synthesis to specific channel requirements.

According to studies [7–12], odd-length Barker sequences have unique autocorrelation properties, which makes them promising for increasing the S/N ratio, and, accordingly, the noise immunity of broadband signals in HF communication systems. However, until now, the issues of determining the optimal Barker sequence for modulating a narrowband signal in order to effectively expand it and increase the S/N ratio in noisy channels has remained unresolved. The quantitative interdependence between the structure of Barker code sequences, specific signal losses in the channel, and the transmission range of broadband signals has also not been sufficiently studied. There is no systematic data on the dependence of S/N ratio on the length of the Barker code (5 and 13 bit) in actual communication channels, taking into account variations in the transmitter output power and specific signal level losses in the communication system.

Some issues related to the processing and recovery of the modulated signal in order to increase the S/N ratio by using various technologies and hardware are given in the papers discussed below.

According to [13], pulse compression technologies, in particular based on modulation, have been successfully used in radar systems for a long time. Due to the ability to increase the S/N ratio and, accordingly, noise immunity, these methods are gradually finding application in analog HF communication systems. The work indicates that pulse compression technology makes it possible to transmit long pulses with low peak power, providing energy advantage and time resolution equivalent to narrow pulses with high peak power. However, unresolved issues are related to the influence of side lobes of matched filters on the signal resistance to interference and the accuracy of its processing in environmental conditions. The reason is the limitation of classical pulse compression algorithms, which is solved by devising new methods for reducing the level of side lobes and using modern adaptive matched filters.

In [14], the concept of waveform diversity is reported; the degree of their influence on the efficiency of radar and analog HF signal transmission systems is established. It is shown that by varying the types of waveforms, it is possible to increase the resolution, improve the adaptability and noise immunity of the systems, as well as optimize signal parameters according to different environmental conditions. However, the issues related to the hardware implementation of the presented solution in analog HF communication systems and the influence of side lobes on the accuracy of signal processing remain unresolved. The reason is the complexity of generating broadband LFM signals, the functional limitation of classical matched filters, and the need to adapt existing algorithms to real operating conditions of the environments.

In [15], a methodology for estimating the angle of arrival of broadband LFM signals based on the cross-correlation of signals received by different channels of an analog communication system is proposed. This approach makes it possible to improve the accuracy of determining the specified angle and the resistance to noise of the working environment, which logically continues the concept of [14] and provides practical application in analog HF communication systems. The issues of integrating the method into real systems with multiple signal reflection remain open. This is due to hardware limitations and the need to optimize signal processing algorithms.

In [16], the results of studies on the use of complementary phase coding of LFM signals in synthesized aperture systems are reported. This provides an effective reduction in the level of side lobes while maintaining a high compression ratio and resolution. The issues related to the influence of multiple beam reflections, noise, and Doppler shifts, as well as hardware limitations in the generation of broadband phase-coded signals remain unresolved. The reason is the complexity of synthesizing codes with a low level of side lobes.

In turn, the authors of [17] note that the research results reported in [16] have significant limitations in practical application. Instead, they propose using complementary pair codes. It is shown that such codes provide a reduction in the level of side lobes and improve the characteristics of the autocorrelation function. The disadvantages include sensitivity to Doppler shifts. The reason is the instability of the complementary properties of the codes when changing the frequency parameters of the signal.

Another direction for increasing the S/N ratio and noise immunity of broadband signals is to use optimal filters [18]. It is shown that the use of such filters makes it possible to significantly reduce the level of side lobes while maintaining high resolution and minimal main lobe losses. The issues related to the high computational complexity and sensitivity to Doppler shifts remain unresolved, which limits the practical implementation in broadband analog HF systems. The reason is the dependence of the optimal characteristics of the filters on the parameters of the signal and the environment.

An alternative solution to the problem of reducing the side lobe level is to use window functions such as Blackman, Flattop, Henning, or Hamming, after preliminary matched filtering [19]. In particular, the use of a Henning window makes it possible to reduce the side lobe level to values below −40 dB but is accompanied by an increase in the width of the impulse response, for example, to 1.33 units, and a decrease in the amplitude of the main lobe. The limitation of all window functions is a compromise between the signal resolution and the amplitude level of the main lobe. An option for suppressing side lobes can be the use of signal modulation by Barker codes in combination with rational hardware solutions.

This is the approach proposed in [20]. The study proved that signal modulation and the use of integration of the side lobe suppression filter with a matched filter can effectively reduce their level without losing the energy of the main lobe. However, the questions of the adaptability of the method to changing environmental conditions, the influence of Doppler shifts and noise on the efficiency of the filter remain open.

In conclusion, the generalized results of [13–20] demonstrate various effective methods for reducing the level of side lobes in broadband signals but the tasks of their implementation in analog HF communication systems remain relevant. This is due to hardware limitations, the complexity of generating broadband signals, and the need to optimize algorithms for the operating environment.

Increasing the S/N ratio and noise immunity of broadband signals by using various hardware designs is considered in [21–30].

In study [21], the designs of analog low-pass filters for integrated broadband receivers were considered. The influence of structural solutions on the stability and sensitivity of the receiving path was analyzed, and improvements were

proposed to reduce distortions in the HF range. The results are of practical importance for the construction of analog paths with increased filtering requirements, especially under the conditions of broadband modulation and the use of correlation-optimized codes, such as Barker codes. At the same time, the interaction of such filters with spectral expansion devices and signal recovery in complex electromagnetic interference environments was not investigated in the work.

The results of studies on the use of cascaded mismatch filters to reduce side lobes of signals modulated by Barker codes are reported in [22]. It is shown that the modernization of matched filters makes it possible to improve the ratio of peak side lobes and increase the efficiency of signal separation in broadband HF communication systems. However, the issues related to the hardware implementation of such filters in real time and their integration into compact and energy-efficient systems remain unresolved. The reason may be the high requirements for computing resources, the complexity of tuning filters for different code sequences, and power consumption limitations. An option to overcome these limitations is to use adaptive hardware solutions, such as programmable logic integrated circuits of matched filters and the use of compact analog adders for signal processing.

This approach was used in [23], which proposed a low-power analog implementation of a matched filter for DS-CDMA systems, characterized by a consumption of 2.3 mW, high speed, and an average frequency of 16.7 MHz. The design provides effective correlation filtering, noise suppression, and high synchronization speed, which makes it relevant for analog HF communication systems. This is one of the few works that reports a full-fledged analog implementation of a matched filter, which is an important basis for building energy-efficient analog paths. At the same time, the issues of integration with other spectrum expansion schemes and parameter tuning for different code sequences are open.

In [24], the results of studies of a filter with dynamic reconfiguration for pulse compression of broadband signals in analog HF communication systems are reported. It is shown that the use of programmable analog matrices provides flexible and energy-efficient signal processing without the need for synchronization at the receiver. However, the issues of limitations of HF processing and integration into complex systems remain unresolved. The reason is the hardware limitations of the speed and accuracy of matrix components.

Paper [25] is aimed at optimizing matched filters in full-duplex systems to reduce self-interference. An adaptive design is proposed that effectively reduces background noise and improves the S/N ratio through the combined adjustment of coefficients in the analog and digital domains. At the same time, the focus on digital algorithms limits the possibility of applying this approach in fully analog HF communication systems, especially in combination with phase modulations.

In study [26], analog and digital low-voltage matched filters were compared. It was shown that analog implementations provide high speed and efficient signal separation in real time, while digital solutions provide greater flexibility in setting system parameters. However, the optimal choice between analog and digital implementations for broadband HF communication systems with simultaneous requirements for low power consumption and high speed remains unresolved.

A practical approach to the design of broadband power amplifiers is reported in [27], in which a graph-analytical method based on the Smith chart is used for impedance matching. This provides a wide bandwidth, high stability and low losses. The issue of dynamic adaptation of amplifiers to variable loads remains unresolved.

Special attention is paid to the construction of channel paths for communication over power transmission lines [28]. It is shown that broadband modulations increase the bandwidth due to hybrid filtering but the implementation of analog matched filters in the HF range remains problematic due to spectral instability and variable impedance of the lines. The combination of pseudo-random sequences (in particular, Barker codes) with energy-efficient matched filters is promising.

In [29], noise suppression and coding methods for broadband systems are investigated. Emphasis is on the application of Barker codes in CDMA technologies where their autocorrelation properties are particularly usable for the implementation of matched filters.

An innovative approach to processing broadband signals by combining analog parallel processing with a silicon photonic platform is reported in [30]. The proposed architecture, which uses a photonic frequency comb and dynamic phase interference, provides effective signal sampling and parallelization in the analog domain, reducing the requirements for speed and memory. Experimental results confirm the operability of the system for processing radar and communication signals on a single integrated circuit. At the same time, there are limitations associated with the temperature and phase stability of photonic components, the complexity of scaling multi-channel systems, as well as the potential increase in power consumption when integrated with other modules. Our review of the literature [21–30] demonstrates that increasing the S/N ratio, and therefore the noise immunity and transmission range of broadband signals in HF communication systems, can be achieved by improving the designs of hardware and signal processing algorithms.

Despite significant progress in this area, there are no universal hardware solutions capable of enabling stable transmission of broadband signals under conditions of nonlinear distortions, impulse noise, and spectral instability of analog HF communication channels. The influence of the S/N ratio after optimal filtering and restoration to the S/N ratio at the receiver input on the noise immunity and signal transmission range has not been studied. The issues of interaction of matched filters with spectral expansion and signal restoration systems and dynamic adaptation of amplifiers to variable environmental parameters and loads remain unstudied. This justifies the relevance of further research aimed at designing practically implemented hardware systems to increase the S/N ratio, noise immunity, and signal transmission range in modern HF communication systems.

One of the effective approaches to improving the S/N ratio and noise immunity of broadband signals, as well as to designing optimal hardware structures without costly experimental studies, is modeling in the “MULTISIM” environment. The authors of [31, 32] emphasize the high correspondence of modeling results to the experimental data. In work [31], an analog circuit of a low-noise amplifier at a frequency of 2.2 GHz was optimized, which provided a high gain and a low level of intrinsic noise, which is extremely important for the receiving paths of HF systems. The wider capabilities of “MULTISIM” are described in [32] for modeling complex analog circuits, including amplifiers, filters, and generators. It is proven that the environment provides flexible verification of the operation of circuits under different modes.

Our review has revealed that although there are effective methods and hardware to increase the noise immunity and transmission range of broadband signals, the reported results

are mostly reproducible only under the conditions in which the research was conducted. At the same time, the issues of the influence of the S/N ratio and transmitter parameters on the efficiency of broadband transmission remain insufficiently studied. Therefore, there is a task to improve the noise immunity and transmission range of broadband signals in analog HF communication systems by optimizing the reception and modulation parameters of the signal. In particular, this can be achieved by establishing the influence of the S/N ratio gain indicator after optimal processing, power and phase modulation parameters on the noise immunity and transmission range of the signal.

The results could be used to develop and optimize technologies and hardware structures adapted to the operating conditions of analog HF communication systems. They could also be applied to implement modern methods of modeling and processing analog broadband signals in order to improve their noise immunity and transmission accuracy.

3. The aim and objectives of the study

The aim of our work is to enable increased noise immunity and transmission range of broadband signals in analog HF communication systems by optimizing the parameters of signal reception and modulation. This will make it possible to devise technological and technical solutions aimed at improving the efficiency, reliability, and stability of signal transmission in channels with high noise levels and dynamically changing propagation conditions.

To achieve the goal, the following tasks were set:

– to investigate the influence of the ratio of the output to the output S/N levels on the noise immunity of the signal;

– to investigate the influence of the power and phase modulation parameters on the signal transmission range.

4. The study materials and methods

4. 1. The object and hypothesis of the study

The object of our study is analog HF communication systems using broadband signals modulated by the Barker code.

The subject of the study is the regularities of the influence of phase modulation parameters and optimal processing of broadband signals on their noise immunity and transmission range in analog HF communication systems.

The hypothesis of the study assumes that phase modulation of broadband signals with their subsequent optimal processing could provide an increase in their noise immunity and transmission range in analog HF communication systems.

During the study, the following assumptions were adopted:

– the line impedance (R_x = 500 Ohm) is a constant;

– the load resistance and source impedances are unchanged during the study;

– resistive, capacitive, and inductive components are idealized or have constant nominal values without long-term degradation;

– the transmitter and noise parameters are static;

– wave and signal parameters at the input of the module under the ABC 1/3 modes are constant within a series of tests;

– additive noises are considered as random variables with a certain standard deviation, which is described by the normal (Gaussian) law;

– signal and noise flows do not interact inside the module up to the matched filter, i.e., a linear system model is used;

– no additional unpredictable disturbances arise between the matched filter, recovery and modulation stages;

– to assess the noise immunity of the system, a model with the ratio S / W = 1 is used, which corresponds to a typical scenario within the given conditions.

During the research, the following simplifications were accepted:

– linear convolutions and adders with constant coefficients are used for linear approximation of the matched filter and the recovery unit;

– insignificant parasitic effects, such as nonlinear distortions outside the matched filter and modulation distortions outside the given scheme, are neglected;

– approximate models of filters and impulse responses are used to reduce computational complexity and simulation time;

– stable and repeatable signal recovery is ensured by a narrow frequency range and a discrete duration τ_0.

4. 2. Methodology for studying the influence of the ratio of input to output S/N levels on the noise immunity of the signal

In order to verify the proposed technical solution, a laboratory device was designed, shown in Fig. 1.

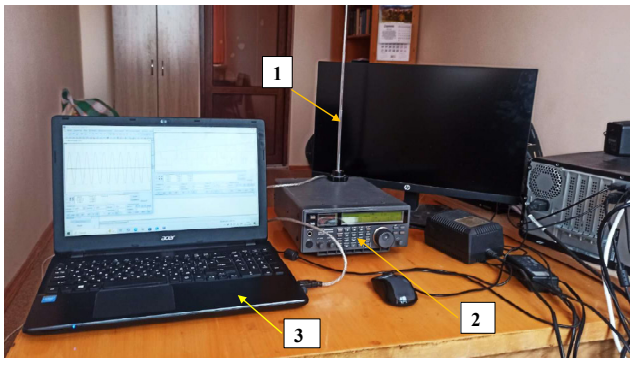

Fig. 1. Laboratory device: 1 – receiving magnetic base antenna mod. ICS-4G/3G/2G-05-M 800-2700 MHz (ICS-TECH company, Ukraine); 2 – receiver for converting the input frequency and forming an analog signal IFAT-2400 (Syntonic Microwave company, USA); 3 – personal computer PC-WIN-6HH1GBUPL4N model Latitude E5470 (Dell company, USA)

The PC (Fig. 1) performs analog signal processing, namely it forms a broadband signal, carries out its optimal processing for forming signals and transmitting them to the data transmission system. To simulate the input signal, a simulation device is used, which contains an ICS-4G/3G/2G-05-M 800-2700 MHz antenna (ICS-TECH, Ukraine) and a Rigol DSG3060 high-frequency signal generator (RIGOL Technologies, China).

The operational principle of the laboratory device was similar to the CDMA principle. All signals were simultaneously transmitted in one frequency band. The signal receiver, by means of correlation processing, isolated a certain message (in coded form) from the specified sender from the message stream. This allowed us to have quite a lot of separate channels in one frequency range that worked without interfering with each other.

In order to study the signal spectrum expansion and restoration unit of an HF communication system with an analog path, a corresponding functional diagram was built: Fig. 2.

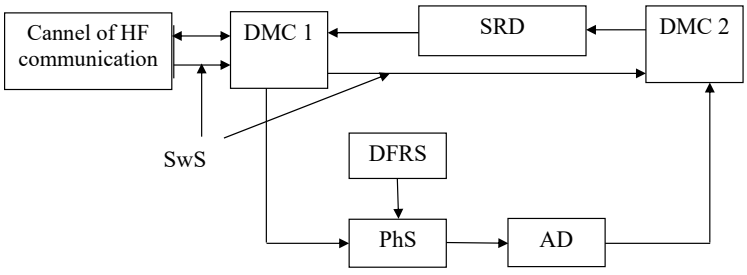

Fig. 2. Functional diagram of the HF communication system signal spectrum expansion and restoration unit with an analog path: DMC 1, DMC 2 – device for matching and controlling the output impedance of the HF communication channel from the expansion and restoration unit; DFRS – device for forming rectangular signals with given parameters; PhS – phase switch for forming a broadband signal (changing the signal phase according to the control signal with given parameters); AD – amplifying device for forming a signal of a given power; SwS – signal for switching the operating modes of the transmitting and receiving paths; SRD – signal recovery device (conversion of a wide-spectrum signal to a narrow-band signal)

The structure of the signal recovery device is shown in Fig. 3.

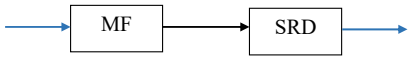

Fig. 3. Module diagram of the signal recovery device: MF – matched filter; SRD – signal recovery device

In this study, MF is a linear optimal matched filter designed according to the spectral characteristics of the desired signal and noise. The main purpose of MF is to detect signals of a given shape against the background of noise. The matched filter for the sequential Barker code $N = 5$ is shown in Fig. 4.

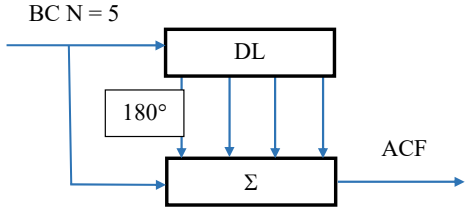

Fig. 4. Matched filter for sequential Barker code $N = 5$: DL – delay line; 180° – signal phase shift, degrees; Σ – signal adder

The module diagram of the device for converting (restoring) a broadband signal into a narrowband (NB) signal to obtain a radio signal with the parameters necessary for HF communication is shown in Fig. 5.

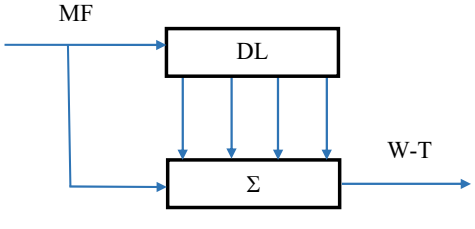

Fig. 5. Module diagram of the signal recovery device: DL – delay line; Σ – signal adder; W-T – walkie-talkie

Optimality is taken to be the degree of achieving the maximum signal-to-noise ratio (S/N) at the filter output. It is worth noting that when the signal passed through the filter, its shape changed.

In order to study the operation of the unit, the following requirements were formulated:

– the duration of the Barker code discreteness had to correspond to the full number of periods of the carrier frequency

$$\tau_0 = (2n+1)/f_{cf}, \quad (1)$$

where τ_0 – duration of the Barker code discrete, μs; f_{cf} – carrier frequency of the signal, MHz; n – number of elements of the Barker sequence;

– duration of the Barker code according to the Nyquist law should be

$$T_{BC} \le \frac{1}{2 \cdot \Delta f}, \quad (2)$$

where T_{BC} is the duration of the Barker code; Δf is the frequency band

$$F = \frac{1}{\tau_0}, \quad (3)$$

where F is the frequency band, Hz.

The noise immunity of a broadband signal according to [33] is

$$q^2 = 2 \cdot B \cdot \rho^2, \quad (4)$$

where q^2 is the S/N ratio at the receiver input;

ρ^2 is the S/N ratio after optimal filtering and restoration;

B is the time-frequency expansion coefficient (the product of the signal duration and its bandwidth, or the processing gain).

Digital values of the input parameters for calculations: $\Delta f = 8$ kHz; $f_{cf} = 4$ MHz. To expand the spectrum band, the Barker code sequence $N = 5$, $\tau_0 = 1$ μs, $T_{BC} = 62.5$ μs was used.

Investigating the efficiency of the HF communication system with an analog path, it was necessary to prove the overall functionality of the designed circuit and its resistance to broadband interference.

4. 3. Methodology for studying the influence of power and phase modulation parameters on the signal transmission range

The electrical diagram of the transmission path of the analog signal spectrum expansion and restoration unit, assembled in the "MULTISIM" workspace, is shown in Fig. 6.

Fig. 7 shows the structure of a matched filter for sequence $N = 5$, implemented as part of the receiving path. The filter circuit contains four DL with a time interval of 1 μs, a differential adder, and implements an impulse response corresponding to a Barker code of length $N = 5$.

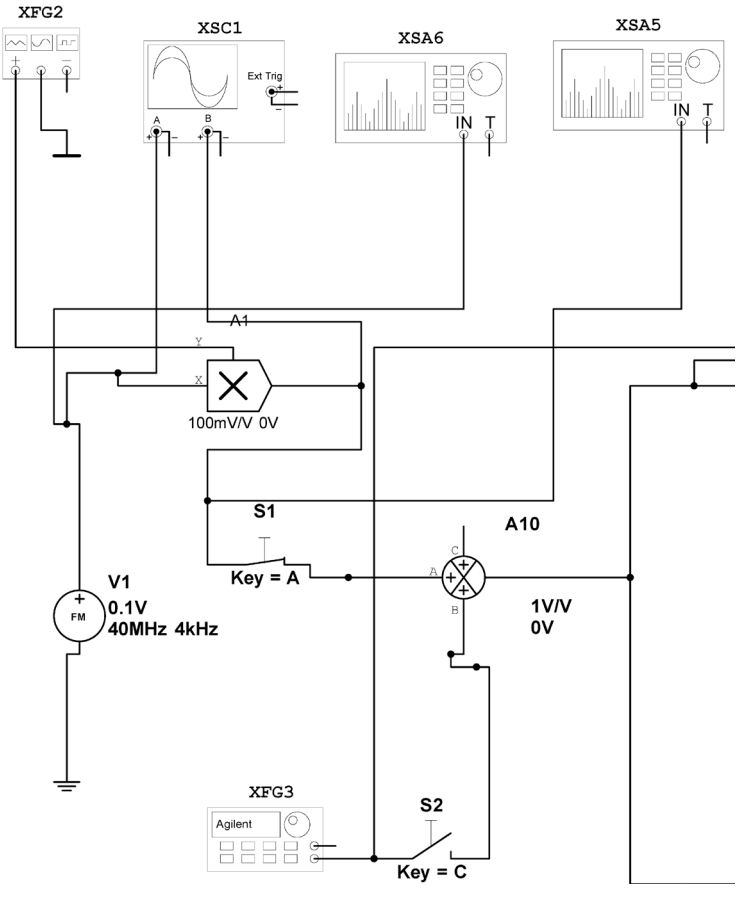

Fig. 6. Electrical diagram of the transmission path of the analog signal spectrum expansion and restoration unit: V1 – radio simulator (carrier frequency f_{cf} = 4 MHz; frequency band Δf = 8(4+4) kHz); XFG2 – functional generator that generates a Barker code sequence N = 5 ((τ_0 = 1 μs); 100 mV/V 0V – radio signal generator with a modulated Barker code sequence N = 5; S1 – switch for connecting the radio signal to the output of the unit; S2 – switch for connecting radio noise to the output of the unit; CAB – signal adder; XSC1 – 4-channel oscilloscope; XSA5, XSA6 – spectrum analyzer; XFG3 – noise generator

A schematic representation of the signal recovery device is shown in Fig. 8.

The developed circuit in Fig. 8 contains four DL, implemented as series-connected elements with a delay of 1 μs each (A6–A9). Therefore, at the input of the adder there are five versions of the signal: the current one and four with time shifts of 1, 2, 3, and 4 μs, respectively. This structure makes it possible to smooth or filter the signal, as well as compensate for distortions that have arisen as a result of previous transmission or processing.

To sum the signals, an adder on an operational amplifier (OPAMP_3T_VIRTUAL element), which has an inverse configuration, is used. Resistors (500 Ohms) at the amplifier inputs form the weighting coefficients of each of the summed signals. Feedback is provided by resistor R2 (10 kOhm), which determines the overall gain of the circuit. To ensure the stability of the amplifier, an additional resistor R4 (2 kOhm) connected to the reference potential is included in the circuit.

The circuit configuration provides the implementation of linear convolutions in signal smoothing tasks in analog information processing devices. Depending on the type of resistors at the inputs, one can set different impulse characteristics of the system, including weighted average smoothing or approximation to the low-pass filter.

In Fig. 9 we show a circuit for checking the operation of the expansion unit and restoring the spectrum of HF signal with an analog path in the "MULTISIM" program (Electronics Workbench, Canada).

Calculations related to the assessment of the change in the transmission range of a broadband signal by HF communication systems when using a recovery unit were performed according to recommendations from [34–36]. For this purpose, a comparison of individual parameters of the information transmission system over power transmission lines was carried out. In particular, the maximum propagation distance of usable signal was determined provided that it attenuates to a level at which the S/N ratio in power will be q^2 = 10 dB: Table 1.

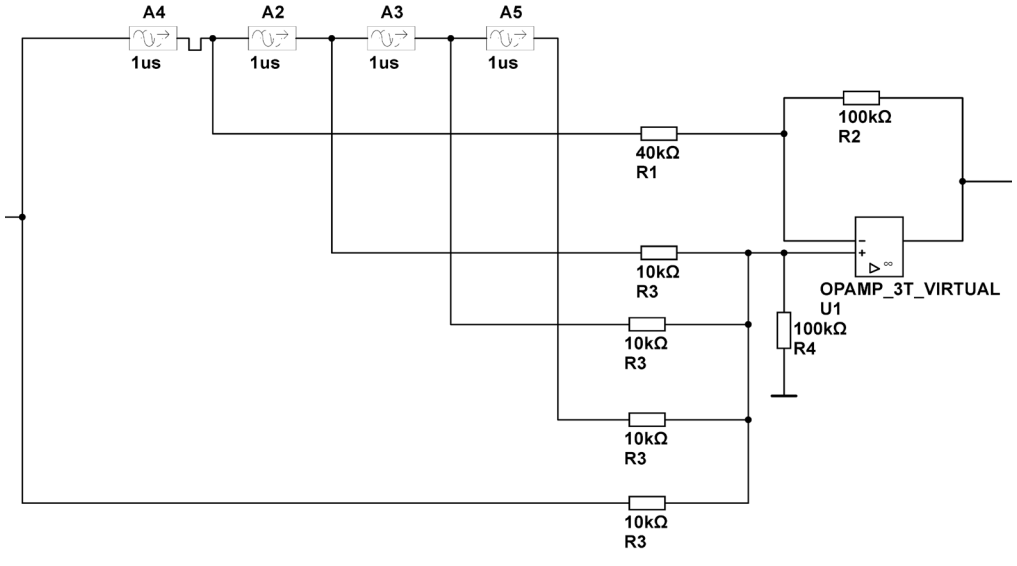

Fig. 7. Schematic representation of a matched filter for sequence N = 5

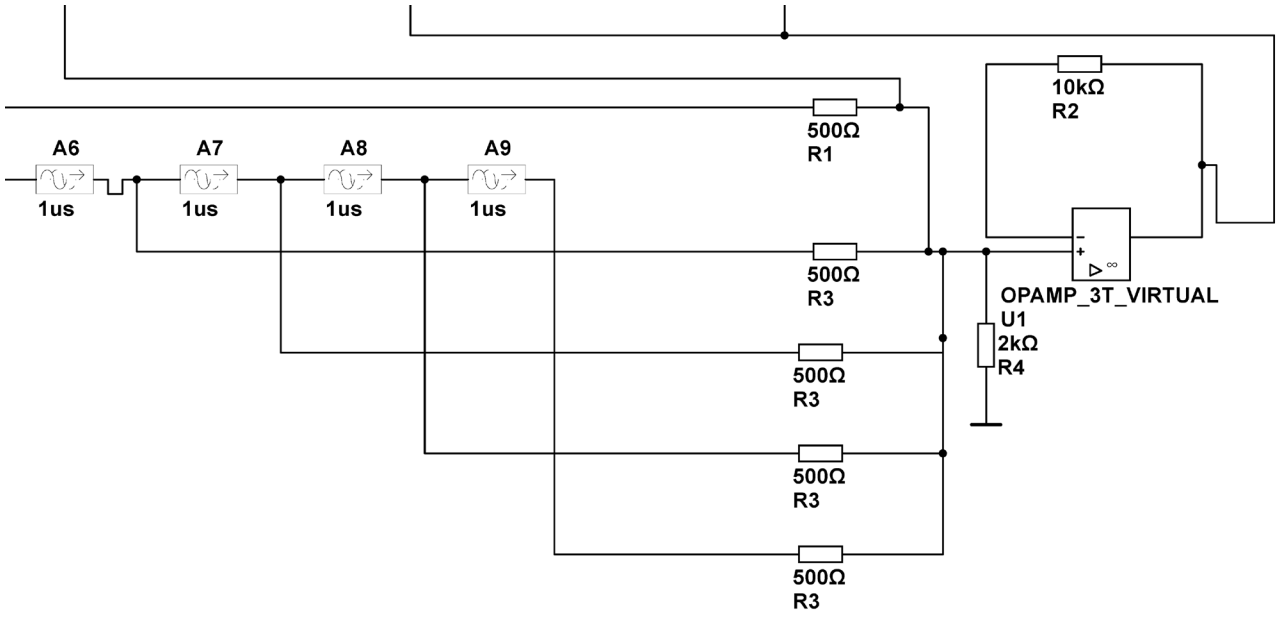

Fig. 8. Schematic diagram of a signal recovery device

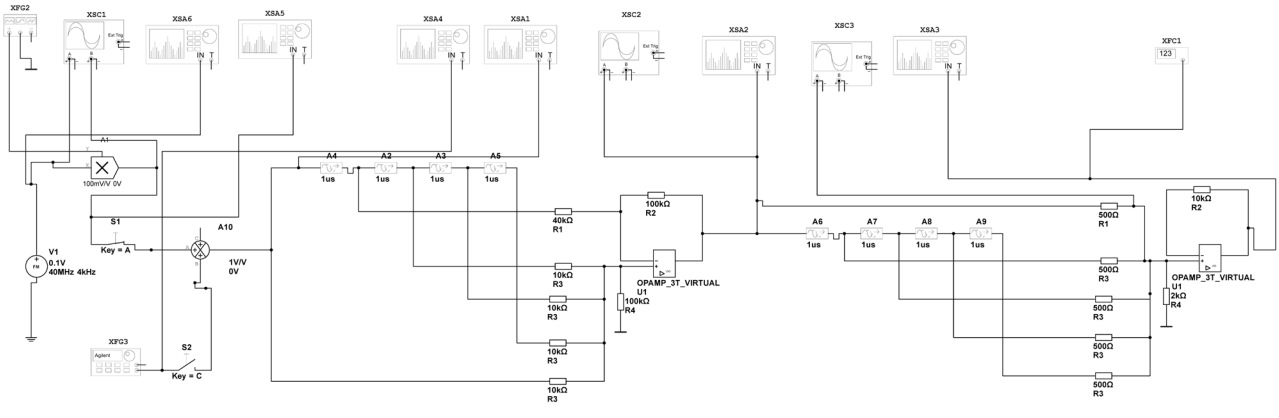

Fig. 9. Scheme for checking the operation of the HF signal spectrum expansion and recovery unit with an analog path in the "MULTISIM" program

Table 1

Basic technical characteristics of systems that transmit information over power transmission lines

ID	ABC 1,3	Siemens HF-PowerLine	Sagem SA-VHF	AEG Telefunken VFT
Manufacturer company	Neptune, Ukraine	Siemens AG, Germany	Sagem, France	AEG/Telefunken, Germany
Telemechanics channel bandwidth (TM), kHz	2.64–3.4	2.5–3.4	2.5–3.4	2.5–3.4
Telephone line bandwidth (TLB) of the channel, kHz	0.3–3.4	0.3–3.4	0.3–3.4	0.3–3.4
Frequency separation, kHz	12–20 (for 3 channels)	$^{3}12$	$^{3}12$	$4 \cdot n$, not less than 8 (n – channel number)
HF channel bandwidth, kHz	4–12	4–12	4–12	4–12
Operating frequencies, kHz	36–108	36–108	40–100	36–108
Number of channels, pcs	1, 3	1–4	1–4	1–4
Power line voltage range, kV	110–1150	110–400	30–300	110–400
Signal generation/processing	Analog / 2nd generation	Analog / 2nd generation	Analog / 2nd generation	Analog / 2nd generation
Transmitter power, W	10, 40, 80	10–20	10–25	10–25

Since the technical characteristics of different systems for transmitting information over power transmission lines are similar, and the difference is only in the different number of channels, for further analysis we choose the ABC 1.3 communication system (manufacturer "Neptune", Ukraine).

The S/N ratio was determined by methodology [37] as the ratio of the signal power (significant information) to the background noise power (unwanted signal), and was calculated from the following mathematical dependence

$$q^2 = \frac{P_s}{P_n} = \left(\frac{U_s}{U_n}\right)^2, \quad (5)$$

where P_s is the signal power, W; P_n is the noise power, W; U_s is the signal voltage, V; U_n is the noise voltage (unwanted signal), V.

The value of signal voltage at $q^2 = 10$ dB is determined from the following expression

$$U_{s_{q^2}} = \sqrt{10} \cdot U_s. \quad (6)$$

According to the methodology from [37], knowing the wave impedance of the power line, it is possible to determine the signal power and amplitude of the signals of communication systems

$$Đ = U^2 / R_x, \quad (7)$$

where P is the signal power, W; U is the amplitude value of the line voltage, V; R_x is the wave impedance of the power line, Ohm.

Signal amplitudes of communication systems

$$U = \sqrt{P \cdot R_x}. \quad (8)$$

Signal transmission range via HF communication

$$D = \frac{P - P_n}{\gamma}, \quad (9)$$

where D is the signal transmission range by HF communication means, m; P_n is the noise power, W; γ is the coefficient characterizing the specific signal level loss by the communication system, dB/m.

It is also known that the maximum range of a radio communication system is

$$D \propto \sqrt{P_n}, \quad (10)$$

The voltage at the transmitter output was found using equation (7) and was 100 V. The dependence of the total attenuation of the power line on the operating frequency was determined using the methodology given in [37].

5. Results of investigating the influence of parameters of the signal and the receiving path on the noise immunity and communication range

5. 1. Results of investigating the influence of ratio of the output to the output S/N levels on the noise immunity of the signal

The noise-resistant broadband signal for analog HF communication systems was formed by modulating a narrowband signal with a five-bit Barker code with subsequent spectral expansion and restoration and using the time redundancy of information transmission to increase the S/N ratio.

Fig. 10 shows the diagrams of the transmission path. In the HF communication system, the transmission path was activated by a control signal (CS), which passed through the matching and output impedance control devices of the channel DMC 1 and DMC 2 (Fig. 2). The carrier frequency signal (Fig. 10, *a*) and a five-bit Barker video code with specified parameters (Fig. 10, *b*) were fed to the input of the phase switch. As a result of the multiplication of diagrams (Fig. 10, *a, b*), a radio signal with an expanded spectrum (Fig. 10, *c*) was formed, which is a necessary condition for correlation extraction. This signal has a frequency band F which is equal to $F = 1 / \tau_0$.

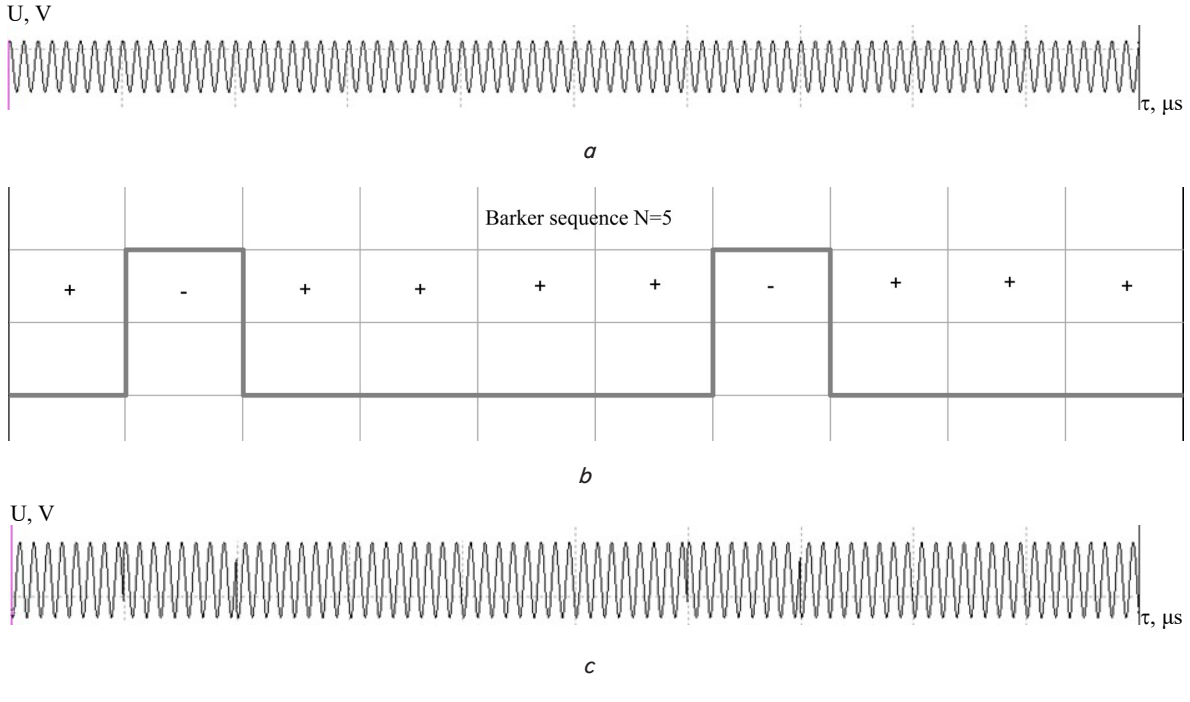

Fig. 10. Diagrams of the transmission path of the module: *a* — input signal; *b* — five-bit Barker code fed to the phase modulator; *c* — radio signal modulated by a Barker code of length $N = 5$

In the diagrams (Fig. 10), the signs "+" and "–" correspond to the amplitude levels of the Barker code elements with a length of $N = 5$. They form a periodic sequence that acts as an excitation signal for the correlation filter, enabling correct signal detection against a background of noise.

Under the reception mode, control signal (CS) received at DMC 1 activated the receiving path of the antenna set-top box. The received signal passed through DMC 2, where it was pre-amplified, after which it was fed to module SRD. In the SRD module, the signal underwent matched filtering. The matched filter (Fig. 4) was optimized for the spectral characteristics of the Barker code, which ensured the achievement of the maximum S/N ratio.

To assess the noise immunity, the autocorrelation function (ACF) of the Barker code sequence $N = 5$ was calculated. The work of MF, namely the calculation of the autocorrelation function of the Barker code sequence $N = 5$, is represented in the form of a rhomboid-like Table 2. In Table 2, (BC) + + + – + is the Barker code $N = 5$ and (Ir) + – + + + is the impulse response of the Barker code N = 5.

Table 2

Calculating the autocorrelation function of the Barker code sequence $N = 5$

BC / Ir	+	+	+	–	+	0	0	0	0
+	+	+	+	–	+	0	0	0	0
–	0	–	–	–	+	–	0	0	0
+	0	0	+	+	+	–	+	0	0
+	0	0	0	+	+	+	–	+	0
+	0	0	0	0	+	+	+	–	+
ACF	+	0	+	0	5+	0	+	0	+

Since in Table 2 the ACF calculations were performed for the single Barker code $N = 5$ while the studies assume constant code repetition, the next step was to determine ACF of the periodic Barker code (Table 3).

Table 3

Calculating the autocorrelation function of the periodic Barker code $N = 5$

1	+	0	+	0	5+	0	+	0	+	0	0	0	0	0	0	0	0	0	0	0	0	0	0
2	0	0	0	0	0	+	0	+	0	5+	0	+	0	+	0	0	0	0	0	0	0	0	0
3	0	0	0	0	0	0	0	0	0	0	+	0	+	0	5+	0	+	0	+	0	0	0	0
4	0	0	0	0	0	0	0	0	0	0	0	0	0	0	0	+	0	+	0	5+	0	+	0
ACF	+	0	+	0	5+	+	+	+	+	5+	+	+	+	+	5+	+	+	+	+	5+	+	+	+

The waveform at the output of the matched filter is shown in Fig. 11.

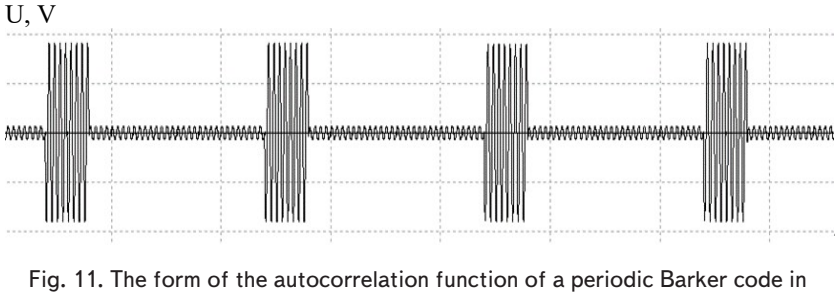

Fig. 11. The form of the autocorrelation function of a periodic Barker code in steady state

The obtained АКФ form (Fig. 11) confirmed the presence of a sharply pronounced main peak with minimal lateral deviations. This provides high selectivity under conditions of interference.

The next stage of the study was associated with signal recovery. The principle of operation of the signal recovery device is given in Table 4 and shown in Fig. 12.

Table 4

Narrow-spectrum signal formation

5+	+	+	+	+	5+	+	+	+	5+	+	+	+	5+	+	+	+
+	5+	+	+	+	+	5+	+	+	+	5+	+	+	+	5+	+	+
+	+	5+	+	+	+	+	5+	+	+	+	5+	+	+	+	5+	+
+	+	+	5+	+	+	+	+	5+	+	+	+	5+	+	+	+	5+
+	+	+	+	5+	+	+	+	+	+	+	+	+	+	+	+	+
9+	9+	9+	9+	9+	9+	9+	9+	9+	9+	9+	9+	9+	9+	9+	9+	9+

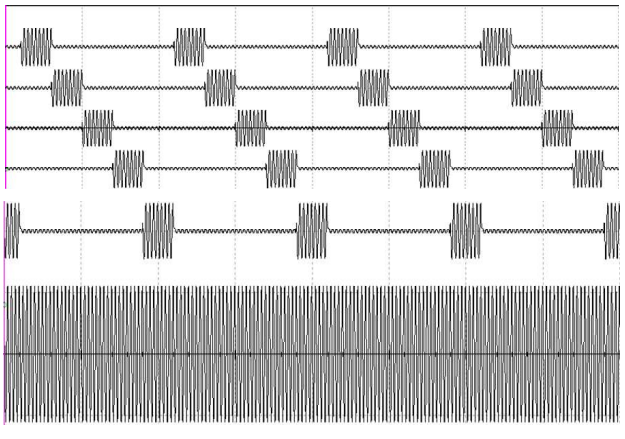

Fig. 12. Radio signal recovery diagrams

The radio signal from MF output is branched into several parallel paths and fed to DL taps, where each subsequent signal is delayed by an interval τ_0 relative to the previous one. After that, the signals are coherently summed, forming a radio signal with a narrow spectrum that is fed to the radio station input for further transmission via the HF communication channel. The amplitude spectrum of the signal is characterized by the presence of a dominant main peak with an amplitude of 9 units, while the side lobes do not exceed 1 unit, i.e., approximately nine times smaller than the maximum. The width of the main peak is about 1–2 μs, which corresponds to the time resolution for correlation separation.

Thus, the spectrum of the radio signal of the radio station was expanded to $F = 1 / \tau_0 = 1/10^{-6} = 1$ MHz (at the level of 0.5). The spectrum is wide, discrete, which meets the requirements. Using DFRS, one can control the duration and number of discretes, on which the spectrum width and its density depend. When receiving a signal with a wide spectrum, the signal is restored in the antenna set-top box and transmitted to the input of the HF receiver.

The noise immunity of a broadband signal is determined from relationship (4), which describes the relationship between the S/N ratio after optimal filtering and restoration and the S/N ratio at the receiver input. Studies on the noise immunity

of amplitude-modulated (AM) signals (without phase modulation; with phase modulation by a five-bit Barker code; by a thirteen-bit Barker code) are illustrated in Fig. 13.

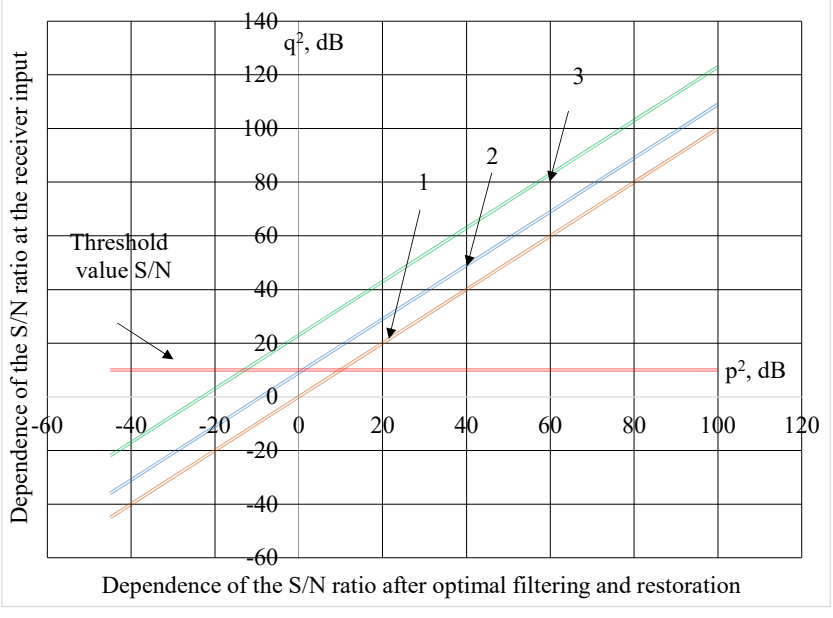

Fig. 13. Dependence of the S/N ratio after optimal filtering and restoration (p^2) on the S/N ratio at the receiver input (q^2): 1 — AM signal without phase modulation; 2 — AM signal with phase modulation by a five-bit Barker code; AM signal with phase modulation by a thirteen-bit Barker code

The graphical dependences shown in Fig. 13 demonstrate a significant increase in the noise immunity of broadband AM signals depending on the type of phase modulation used. The base signal without phase modulation (curve 1) is characterized by a relatively low S/N ratio at the receiver input: to achieve a threshold value of 10 dB, the S/N ratio must be over 20 dB. This means that with a S/N ratio at the receiver input of 0 dB, the probability of correct signal detection does not exceed 0.55. This result correlates with classical analytical estimates of amplitude modulation and demonstrates the limitations of its effectiveness under conditions of high interference.

The use of AM signals with phase modulation by a 5-bit Barker code (curve 2) significantly improves their characteristics. The threshold value is achieved already at 0 dB at the receiver input (the advantage in noise immunity is ≈9 dB compared to the base signal). At the same time, the S/N ratio after optimal filtering and restoration reaches values that ensure correct signal detection with a probability of over 0.8. This confirms the high efficiency of correlation signal processing even under conditions of reduced S/N ratio at the input.

The most pronounced effect occurs when using phase modulation with a 13-bit Barker code (curve 3). In this case, the threshold value of the output S/N ratio, necessary to ensure the specified reception quality, is achieved already at –5 dB at the receiver input, which has an advantage of ≈22 dB over classical AM and ≈13 dB compared to a 5-bit code.

Due to the low level of the side lobes of the autocorrelation function (approximately –22 dB) and high energy efficiency, high-quality reception is ensured even when the signal level is lower than the noise level. For S/N = –5 dB, the probability of correct detection exceeds 0.9, which confirms the significant averaging of noise components and the amplification of the correlation peak.

Increased noise immunity of the broadband signal is provided by a combination of phase modulation with a Barker code, MF and signal recovery through DL. Phase modulation forms a periodic sequence with a sharply pronounced main ACF peak and minimal side lobes, which allows for correlation isolation of the signal from the noise background. MF optimizes the signal spectrum for the Barker code, increasing the output S/N ratio even at a low input value. DL and coherent summation of signals provide energy concentration in the main correlation peak, which significantly reduces the influence of noise components. As a result, the output S/N after optimal processing significantly exceeds the input. This allows for signal detection when its level is lower than the noise level and provides a probability of correct reception of more than 0.9 at an input S/N of up to –5 dB (for a 13-bit Barker code). Thus, a significant advantage in noise immunity is due to both the spectral expansion of the signal and the effect of correlation isolation of signal energy from the noise background.

5. 2. Results of investigating the influence of power and phase modulation parameters on the signal transmission range

In order to determine the efficiency of the signal expansion and restoration unit, the system's ability to provide an increase in the signal transmission range and an increase in the signal/noise ratio while maintaining (reducing) the transmitter power was investigated.

The operation of the transmission path of the analog signal expansion and restoration unit is illustrated by the diagrams in Fig. 14.

A radio station signal (red diagram, Fig. 14) and a periodic Barker code sequence signal with a length of $N = 5$ (middle diagram, Fig. 14) were fed to the input of the signal formation device for Barker code modulation. A modulated signal with specified parameters was formed at the output of the specified device (blue diagram, Fig. 14).

Fig. 15 shows the spectrogram of the HF transmitter signal and the signal at the output of the unit.

The transmission path of the module formed a signal with a broadband discrete spectrum, which is well illustrated in Fig. 15. In particular, Fig. 15, *a* shows the spectrum of the signal of conventional HF communication, while Fig. 15, *b* shows the broadband spectrum of the signal formed by the transmission path of the module.

Below are the results of studying two variants of the module operation, Fig. 16:

1) $f_{cf} = 4$ MHz, frequency band $\Delta t = 8$ kHz;

2) $f_{cf} = 4$ MHz, frequency band $\Delta t = 8$ kHz, S/N ratio = 1.

The results of modeling the first case, when the signal spectrum has a frequency modulation $\Delta f = 8$ kHz and an average frequency $f_{cf} = 4$ MHz, are shown in Fig. 16, *a*.

After passing through the transmission path, the spectrum is expanded (Fig. 16, *b*). This is due to the action of the transmission filter and the modulation features that add high-frequency components. In Fig. 16, *c*, we have the re-

stored signal. Comparison of the spectra in Fig. 16, *a*, *b* confirms that the input spectrum of the high-frequency signal and the spectrum after processing are practically identical. Therefore, the signal restoration system with high accuracy restores the amplitude-frequency structure of the input signal after spectrum expansion in the transmission path. This confirms the high-quality implementation of the matched filter and the signal restoration unit shown in Fig. 7, 8. The presence of a clearly defined carrier and symmetrical sidebands indicates the stability of the frequency modulation; the absence of parasitic harmonics in the spectrum indicates a low level of noise and distortion in the transmission channel.

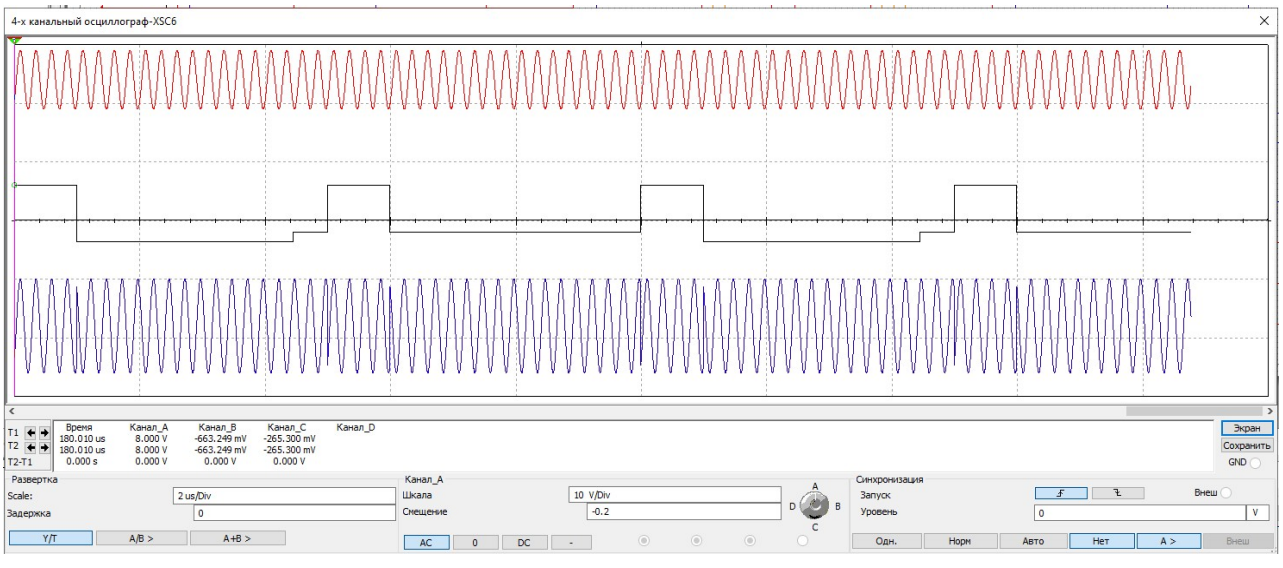

Fig. 14. Diagrams of the transmission path of the module

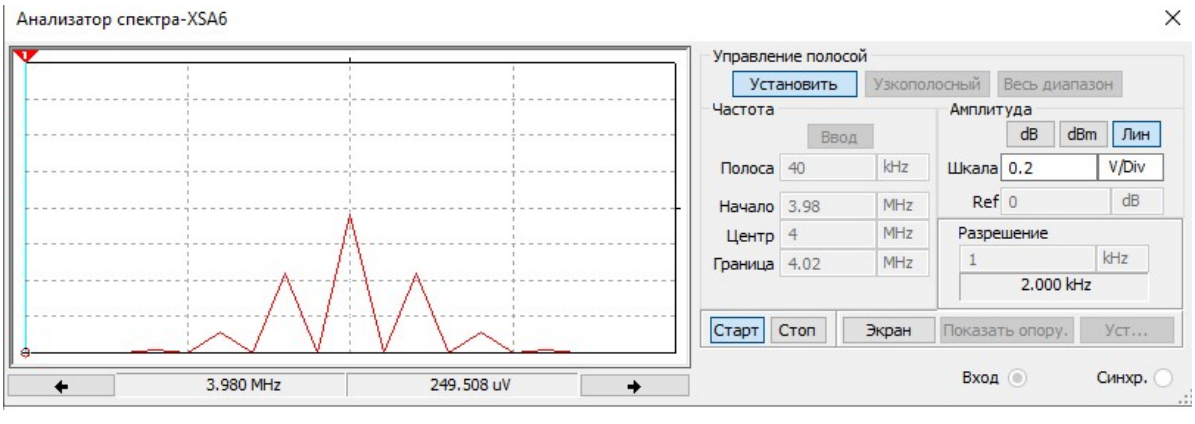

a

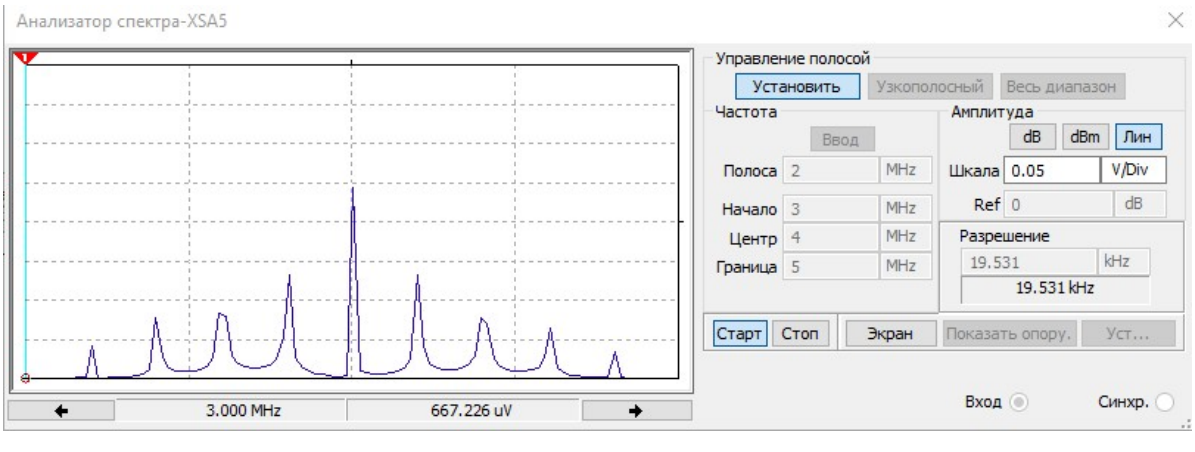

b

Fig. 15. Spectrogram: *a* — HF transmitter signal; *b* — signal at the output of the unit

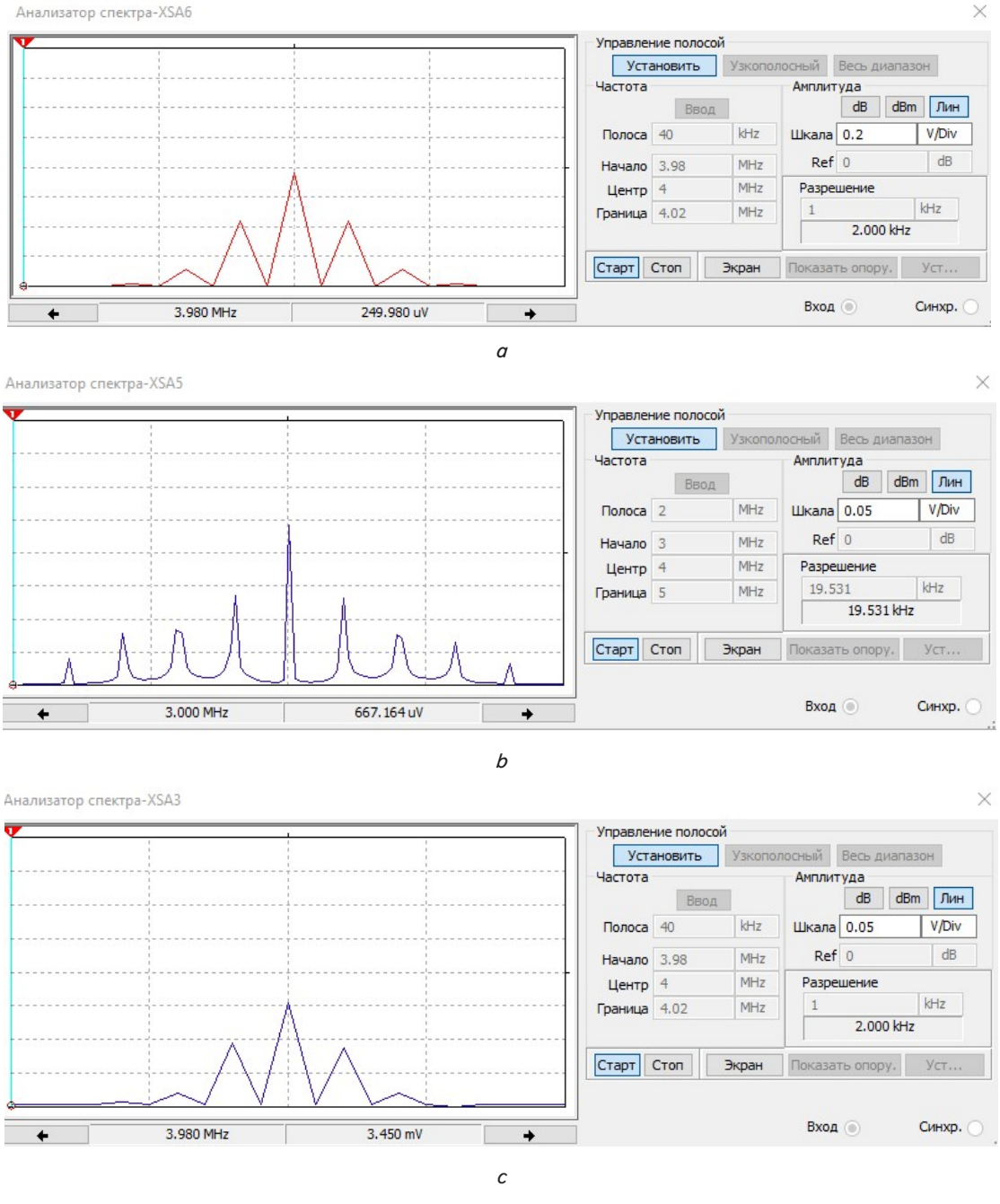

Fig. 16. Spectral characteristic of the signal: *a* — amplitude-frequency characteristic of the signal, which has a carrier frequency $f_{cf} = 4$ MHz, frequency band — $-\Delta f = 8$ kHz; *b* — expanded spectrum of the signal; *c* — restored signal

The second option involved checking the operation of the antenna set-top box in the presence of noise (interference). The HF transmitter generated a radio signal with $f_{cf} = 4$ MHz, frequency band $\Delta f = 8$ kHz, and a S/N ratio of 1. The spectrograms of the HF signal and the restored signal under noise conditions according to the second option are shown in Fig. 17.

Fig. 17, *a* is a spectrogram of the signal at the output of the HF path. The visualized signal has a clearly defined carrier frequency and sidebands, which are formed in accordance with the structure of the transmitted information signal. In this case, the spectral density of the noise is equal to the average value of the signal energy. Some blurring of the spectral lines is observed in the spectrogram, which is due to the presence of noise, but the general structure of the spectrum remains recognizable. Fig. 17, *b* shows the spectrum of the signal after modulation (spectrum expansion). According to Fig. 17, *b*, the spectral structure of the signal is preserved, and the location and intensity of the main components coincide with the original spectrum. Minor deviations in the amplitude and shapes of the peak functions are explained by the influence of additive noise and the limited bandwidth of the system elements.

A comparison of the spectrograms in Fig. 17, *a*, *b* reveals that the signal processing system effectively suppresses the influence of interference, ensuring signal recovery with high accuracy. Although the S/N level is not perfect, the spectrogram of the reconstructed signal clearly reflects the characteristic frequency components inherent in the transmitted message. This indicates the system's resistance to additive noise and confirms the effectiveness of the matched filter and the reconstruction device.

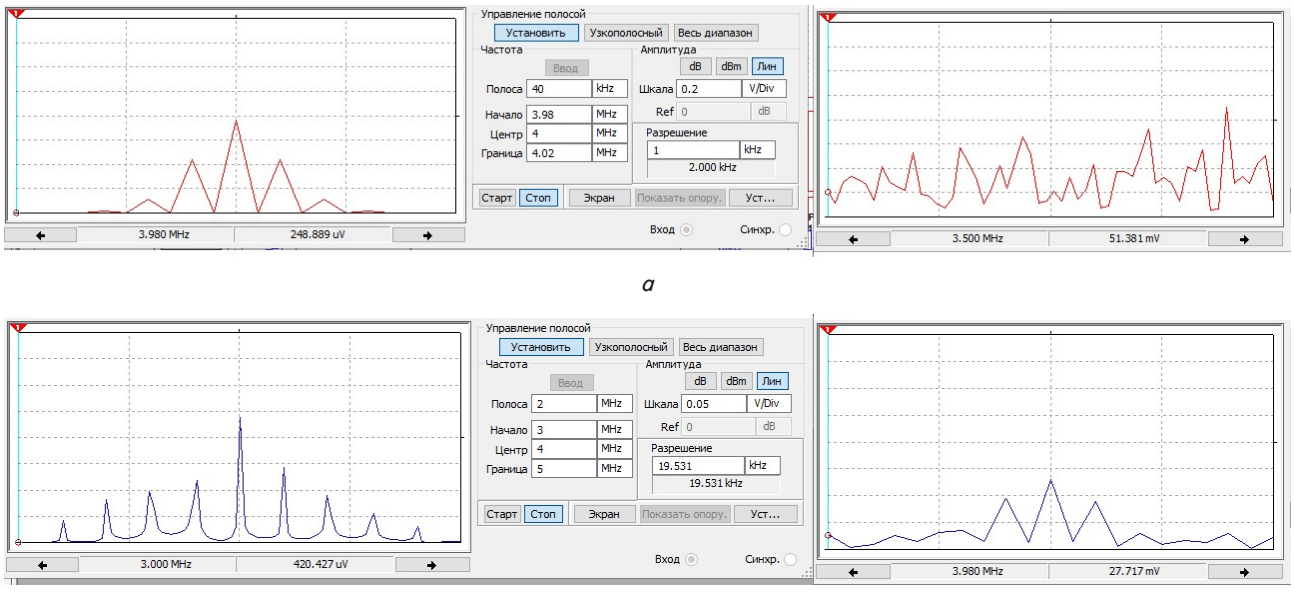

Fig. 17. Spectrograms of the HF signal and the restored signal under noise conditions: *a* – spectrogram of the signal at the HF output at S/N = 1; *b* – spectrogram of the restored signal after phase modulation

Table 5 gives calculations of the influence of the operating frequency on the specific signal level losses by the communication system when transmitting it over power transmission lines. To confirm the reliability of the calculations using the model, the resulting communication characteristics were compared with the technical characteristics of signal transmission systems over power transmission lines given in Table 1.

Table 5

Dependence of the total attenuation of a signal transmitted by the power line on the operating frequency

Operating frequency, (Hz)	Specific loss of signal level by communication system (dB/m)
500	$18 \cdot 10^{-5}$
1000	$28 \cdot 10^{-5}$
1500	$50 \cdot 10^{-5}$
5000	$100 \cdot 10^{-5}$

As a result of our study, it was found that at a noise voltage of 1 V, the value of the noise power (at $q^2 = 10$ dB) was $P_n = 0.02$ W. The maximum transmission range of the power line signal at the operating frequency of the communication medium of 5000 Hz according to mathematical dependence (9) was 19980 m. Knowing the value of the wave impedance of the power line, the following parameter values were substituted into dependence (9): power of the transmitters of the communication systems – 20 W; specific loss of the signal level of the communication system $100 \cdot 10^{-5}$ dB/m. Calculations were performed for the operating frequency of 5000 Hz.

Having performed optimal processing and restoration of the signal, the S/N ratio in power increased by 25 times. Taking into account the proportionality of the range to the square root of the signal power (10), the maximum signal transmission range also increased by $D_5 = (25)^{1/2} \cdot D = 5 \cdot D$. Whereas the initial range was 19980 m, after processing it became $D_5 = 5 \cdot 19980 = 99900$ m. Thus, the communication range increased by 5 times without changing the reception quality.

Analysis reveals that an increase in the S/N ratio by voltage by 5 times is equivalent to an increase in the same indicator by power by 25 times according to quadratic dependence (5). Therefore, it is possible to reduce the transmitter power by 25 times (to $P = 0.8$ W) without losing the functional characteristics of the communication system as effective processing compensates for the decrease in the transmitted energy.

Thus, the designed device can be used for:

– reducing the transmission power without deteriorating the basic communication parameters;

– increasing the range of communication systems while maintaining energy efficiency;

– ensuring secure data transmission, improving electromagnetic compatibility (EMC) and reducing the level of radiation;

– reducing the overall weight parameters of the equipment due to simplifying energy requirements.

Fig. 18 shows the dependence of signal transmission range on the transmitter power at different coefficients characterizing the specific losses of the signal level by the communication system and phase modulations by Barker codes (0, 5, 13).

Fig. 18 shows the dependence of signal transmission range on the transmitter output power at different coefficients characterizing the specific signal level losses by the communication system and phase modulations using Barker codes (0, 5, 13). The specific signal level losses by the communication system are determined by a number of factors, including the type of power line, the thickness of the conductors, the material from which they are made, and the signal carrier frequency. The signal transmission frequencies in the HF channels of power transmission lines are usually in the range of 20–1000 kHz although higher frequency values can be used for household Powerline technologies (2–34 MHz). Narrow frequency bands with a width of about 4 kHz are allocated for signal transmission and frequencies for channel compaction in the range of 27–600 kHz are also used.

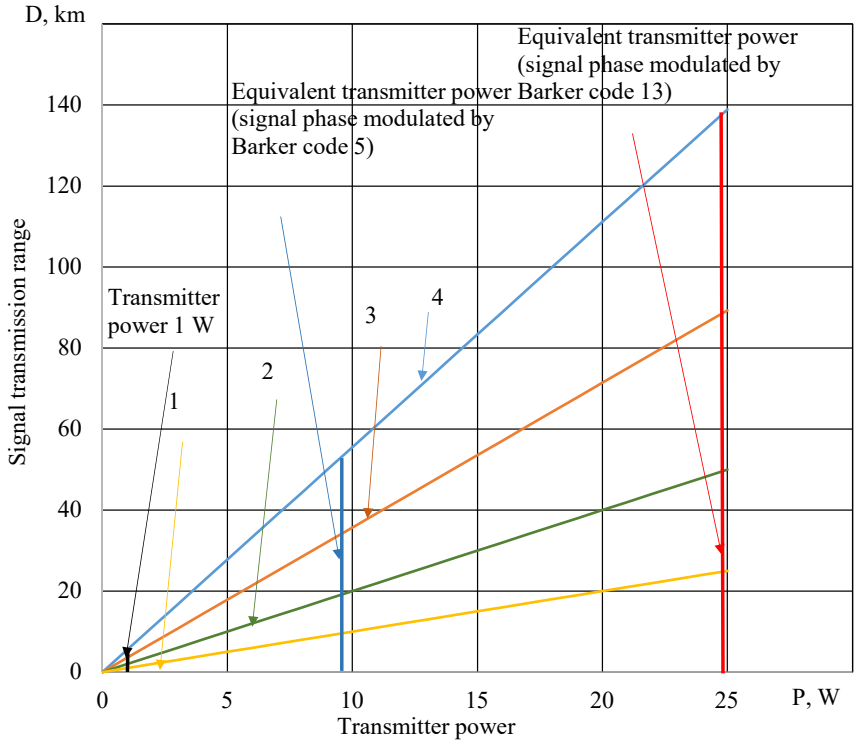

Fig. 18. Dependence of signal transmission distance on the transmitter power at different coefficients characterizing the specific signal level losses by the communication system and phase modulations by Barker codes (0, 5, 13): $1-\gamma=18\cdot10^{-5}$; $2-\gamma=28\cdot10^{-5}$; $3-\gamma=50\cdot10^{-5}$; $4-\gamma=100\cdot10^{-5}$

To establish the dependences (Fig. 18), the concept of equivalent transmitter power is introduced. This term is understood as the output power of a signal without phase modulation at which the same communication range is achieved as in the case of using phase modulation and optimal correlation signal processing. Fig. 18 shows segments perpendicular to the power axis (1, 9, and 25 W), which intersect the lines of dependence of the signal transmission range on power for different values of γ. The intersection points correspond to the communication range for different types of signals.

According to the results, at a power of 1 W, the transmission range of the unmodulated signal was only 5.5 km, while when using the five-bit Barker code it increased to 50 km (an increase of nine times). When using the thirteen-bit code, the range reached 138 km, which is 25 times higher than the base value. Further increases in power to 9 and 25 W provided a proportional increase in absolute range, but the relative increase from the use of Barker codes remained constant. For example, at 9 W, the transmission range of the unmodulated signal was about 49 km, while when using the thirteen-bit Barker code it reached 415 km.

6. Results of investigating the influence of signal and receiving path parameters on noise immunity and communication range: discussion

The results of our study of noise immunity of broadband signals of analog HF communication systems are shown in Fig. 10–12. According to Fig. 10, 12, the formation of the expanded spectrum of the signal at the transmitter input is provided by modulating the transmitted signal with the Barker code. For systems with an expanded spectrum, such a signal structure is typical, which ensures effective separation of the usable signal from the noise background. The Barker code, according to the results from internal correlation analysis (Tables 2, 3), provides a pronounced maximum of the autocorrelation function at zero offset. Even at a low S/N ratio, this contributes to the effective use of MF (Fig. 4) for signal detection. This proves the possibility of coherent signal reception, which is critically important for systems with an expanded spectrum.

Based on the results of our study (Fig. 11, 12), at the signal reception stage, the signal recovery device performs coherent addition of multi-channel taps of the delayed signal. This makes it possible to reduce the spectrum band and match the signal with the parameters of analog HF communication channels. The output signal spectrum (Fig. 12) after processing has a width of up to 1 MHz (at a level of 0.5). This indicates the presence of broadband characteristics of the formed signal. As a result, the multiphase shaper provides adaptive spectrum control in accordance with the specified conditions.

Based on the diagrams (Fig. 10, 12) and the form of the autocorrelation function (Fig. 11), we note that the autocorrelation peak (+5) with minimal sidelobes (0) at $N = 5$ agrees with the classical Barker criterion. The degree of agreement is high. The obtained spectrum width (about 1 MHz) confirms the effective signal expansion, similar to CDMA systems, with the subsequent possibility of compression to a narrowband format at the reception stage. The transmission reliability increases significantly when the transmitted signal is amplified.

Similar to those reported in this work, the results of scientific research [8–10] in the field of Barker code modulation confirm the importance of the ratio of code length and the level of immunity to interference. In work [8], an analysis of the autocorrelation characteristics of the Barker code is carried out. The authors note that among the classical PN sequences Barker has the lowest side lobes and the best selectivity for DSSS/CDMA in network environments. In [9], new composite Barker codes (length 49, 77, 121) were investigated. The authors note that the Barker code $N = 13$ demonstrates the best autocorrelation properties among short sequences. This indirectly confirms the validity of using phase modulation by Barker codes in systems with limited frequency resources. The authors of study [10] demonstrated the high efficiency of using matched filters at low signal levels in multipath propagation conditions. The results shown in Fig. 10–12 coincide with their conclusions regarding the need for high correlation selectivity.

Analysis of the dependence of output S/N after optimal filtering and recovery on input S/N at the receiver (Fig. 13) revealed that the use of Barker codes increases the noise immunity of the signal. The use of a 5-bit code makes it possible to reach the threshold of correct reception at an input S/N of

0 dB. For a 13-bit code, the threshold is achieved even at an input S/N = –5 dB. This provides a significant advantage in noise immunity, and the probability of correct signal detection is more than 0.9. The resulting patterns make it possible to optimize the parameters of the code and hardware implementation, ensuring effective information transmission even at low input S/N.

The results of investigating the efficiency of the signal spectrum expansion and recovery unit by modeling in "MULTISIM" are shown in Fig. 14–18.

Fig. 14 shows the results of modeling the operation of the transmission path of the signal formation unit modulated by the Barker code, with length $N = 5$. The red diagram is the carrier frequency in the form of a harmonic sinusoidal signal. The amplitude of the signal is $A_n \approx 2$ V. The phase of the signal is invariant in time and serves as the basis for the subsequent modulation process. The black diagram is a digital signal that corresponds to the Barker code with length $N = 5$: (+1, +1, +1, –1, +1). The signal values take the levels of 0 V and 1 V. The code sequence determines the instantaneous value of the phase shift of the carrier signal, providing phase modulation. The blue diagram is a modulated signal, i.e., the result of the product of the red and black diagrams. Note that in the interval where the code is "–1", the sinusoid is inverted, i.e., a phase shift of 180° occurs. Thus, modulation is implemented.

As shown in Fig. 15, the spectrogram of the signal after formation has a characteristic broadband structure (Fig. 15, *b*) compared to the narrowband spectrum of a conventional HF transmitter (Fig. 15, *a*), which proves the efficiency of the modulation. The matched filter (Fig. 4) and the signal recovery device (Fig. 5) provide high-precision reproduction of the amplitude-phase characteristics of the input signal after its passage through the transmission path. This is confirmed by the simulation results (Fig. 16): the amplitude-frequency characteristic of the recovered signal (Fig. 16, *c*) is practically identical to the spectrum of the original signal (Fig. 16, *a*), despite the phase-frequency changes introduced as a result of the spectrum expansion in the transmission path (Fig. 16, *b*). Thus, the restored signal retains the carrier frequency $f_{cf} = 4$ MHz and symmetrical sidebands corresponding to the frequency band $\Delta f = 8$ kHz.

In the second considered case, under condition S/N = 1, the spectral structure of the signal is partially distorted (Fig. 17, *a*). However, after its restoration (Fig. 17, *b*), the key components of the spectrum are preserved. Minor changes in amplitude are explained by the influence of noise and a limited bandwidth but overall, the system demonstrates high resistance to additive interference.

Comparison of results at different coefficients characterizing specific signal level losses by a communication system (Fig. 18) showed that with increasing losses, the absolute information transmission range decreases. At the same time, the stable advantage of phase modulation with Barker codes remains: the effect of increasing the signal transmission range is manifested regardless of the level of attenuation in the channel. This indicates the universality of the approach and high noise immunity of signals with Barker codes even in noisy conditions.

The physical essence of the revealed pattern is explained by the features of correlation signal processing. An AM signal in a noisy environment quickly loses its reproduction reliability since the S/N ratio is determined exclusively by the energy parameters of the signal and does not have additional mechanisms for increasing noise immunity. In contrast, phase modulation using Barker codes forms a signal with high temporal structuring, which increases its correlation recognizability and makes it possible to effectively isolate usable information in noisy conditions. Due to the properties of Barker codes – high autocorrelation function and low level of side lobes – the receiver can perform effective correlation processing, which significantly increases the S/N ratio after filtering. This ensures reliable signal separation even against the background of intense interference. In particular, at a transmitter output power of 1 W, the signal transmission range increased by 9 times for the 5-bit Barker code and by 25 times for the 13-bit Barker code compared to the unmodulated signal. Thus, the increase in the signal transmission range is due not only to the additional transmitter power but also to a more efficient use of signal energy due to the optimal structure of the phase-modulated signal.

The results reported in this study are consistent with the results from work [11], which studied the convolution of the Barker and Golay codes for low-voltage ultrasonic testing. Despite the differences in technical implementations, the results in [11] confirm the general trend – correlation processing of code signals significantly increases S/N at low signal levels. And although the use of the Golay code made it possible to extend the sequence and obtain a better main peak, the use of the Barker code $N = 5$ provided a simple, effective hardware implementation for analog HF communication systems with a moderate spectrum width (≈1 MHz).

Thus, our results demonstrate that the use of Barker code modulation together with matched filtering provides a significant increase in the level of noise immunity and the efficiency of using the frequency resource in analog HF communication systems. The implementation of broadband transmission with subsequent recovery in a narrowband format is an effective way to increase the spectral efficiency of such systems.

These results are new in terms of the targeted use of Barker code signal modulation to increase the transmission range of an analog broadband signal and improve the overall noise immunity of HF communication channels.

The practical significance of our research results relates to the possibility of their use for power line data transmission systems, where the use of spread spectrum codes ensures signal transmission at a high level of electromagnetic interference. This technique could be used for covert information transmission, which complicates unauthorized actions by attackers.

A limitation of the research is the use of idealized models of electronic components in a computer simulation environment that do not take into account parasitic parameters (capacitances, inductances, resistances of conductors and contacts). These parameters may significantly affect the behavior of the circuit under real operating conditions. In addition, conducting signal analysis only for the Barker code ($N = 5$) limits the generalization of the results to longer codes.

The disadvantages include the limited length of the Barker code. This reduces the potential for noise immunity in multipath environments (more complex channels will require longer codes or sequences with better autocorrelation properties). Also, the simulation performed in the MULTISIM program does not take into account all the nonlinearities of a real radio channel (including impulse interference, phase noise, grounding effects, etc.). There is also insufficient analysis of long-term effects in the case of long-term signal

propagation, for example, changes in temperature, humidity, or power.

Further research should involve conducting experimental studies, as well as integrating the proposed approach with CDMA, OFDM, and Smart Grid technologies. This will open up the possibility of devising hybrid solutions that combine high noise immunity with rational use of the frequency resource.

7. Conclusions

1. Our study on the influence of the ratio of input and output S/N on the noise immunity of a broadband signal showed that phase modulation by the Barker code in combination with optimal processing significantly increases the signal's resistance to noise interference. The signal modulated by a 5-bit code has a spectral width of 1 MHz, an amplitude of the main peak of the autocorrelation function of 9 units, and a time resolution of 1–2 μs, which ensures effective correlation separation of the usable signal. The threshold value of correct reception for this signal is achieved at input S/N = 0 dB, providing an advantage in noise immunity of about 9 dB compared to the base signal without modulation. The use of a 13-bit code makes it possible to achieve a threshold value of 10 dB already at S/N = −5 dB with a probability of correct signal detection of about 0.9, providing an advantage in noise immunity of 22 dB. The output S/N ratio after optimal filtering and restoration significantly exceeds the input S/N ratio at the receiver, which ensures reliable signal separation in a noisy environment. Our results confirm the effectiveness of phase modulation with the Barker code for increasing the noise immunity of broadband signals and determining the trade-off between code length, hardware complexity, and S/N gain.

2. Simulation in "MULTISIM" has confirmed the efficiency of the signal spectrum expansion and recovery unit using the Barker code ($N = 5$), which forms a broadband discrete spectrum with a width of about 1 MHz. A matched filter and an adder with an inverse configuration ensured effective signal recovery even under conditions of S/N = 1.

At a transmitter output power of 1 W, the transmission range of an unmodulated signal was 5.5 km. Signal modulation with a 5-bit Barker code increased it to 50 km (9 times) and with a 13-bit Barker code – to 138 km (25 times). With an increase in transmitter power, the range increased proportionally, while the relative advantage of phase modulation with Barker codes remained unchanged regardless of the specific signal level losses of the communication system. Our results confirm the high effectiveness of this approach for increasing noise immunity and significantly improving the signal transmission range under actual conditions of their propagation.

Conflicts of interest

The authors declare that they have no conflicts of interest in relation to the current study, including financial, personal, authorship, or any other, that could affect the study, as well as the results reported in this paper.

Funding

This paper was supported by the HEI-COPILOT project within the EIT HEI Initiative "Innovation Capacity Building for Higher Education", funded by the European Union.

Data availability

The data will be provided upon reasonable request.

Use of artificial intelligence

The authors confirm that they did not use artificial intelligence technologies when creating the current work.

References

1. Giraneza, M., Abo-Al-Ez, K. (2022). Power line communication: A review on couplers and channel characterization. AIMS Electronics and Electrical Engineering, 6 (3), 265–284. https://doi.org/10.3934/electreng.2022016
2. Del Puerto-Flores, J. A., Naredo, J. L., Peña-Campos, F., Del-Valle-Soto, C., Valdivia, L. J., Parra-Michel, R. (2022). Channel Characterization and SC-FDM Modulation for PLC in High-Voltage Power Lines. Future Internet, 14 (5), 139. https://doi.org/10.3390/fi14050139
3. Girotto, M., Tonello, A. M. (2017). EMC Regulations and Spectral Constraints for Multicarrier Modulation in PLC. IEEE Access, 5, 4954–4966. https://doi.org/10.1109/access.2017.2676352
4. Fan, Z., Rudlin, J., Asfis, G., Meng, H. (2019). Convolution of Barker and Golay Codes for Low Voltage Ultrasonic Testing. Technologies, 7 (4), 72. https://doi.org/10.3390/technologies7040072
5. Ustun Ercan, S., Pena-Quintal, A., Thomas, D. (2023). The Effect of Spread Spectrum Modulation on Power Line Communications. Energies, 16 (13), 5197. https://doi.org/10.3390/en16135197
6. Hernandez Fernandez, J., Jarouf, A., Omri, A., Di Pietro, R. (2023). Inferring Power Grid Information with Power Line Communications: Review and Insights. arXiv. https://doi.org/10.48550/arXiv.2308.10598
7. Schmidt, K.-U., Willms, J. (2015). Barker sequences of odd length. Designs, Codes and Cryptography, 80 (2), 409–414. https://doi.org/10.1007/s10623-015-0104-4
8. Maksimov, V., Khrapovitsky, I. (2020). New composite barker codes in the synchronization system of broadband signals. Information and Telecommunication Sciences, 2, 24–30. https://doi.org/10.20535/2411-2976.22020.24-30
9. Maksymov, V., Noskov, V., Khrapovytsky, I. (2022). New Barker's composite codes as modulation signals in broadband communication systems. Information and Telecommunication Sciences, 2, 15–20. https://doi.org/10.20535/2411-2976.22022.15-20

10. Maksymov, V., Gatturov, V., Khrapovytsky, I. (2022). New composite Barker codes, gold codes and kasamisequences in broadband signal synchronization systems. Information and Telecommunication Sciences, 1, 14–21. https://doi.org/10.20535/2411-2976.12022.14-21
11. Abdel-Rahman, M. A. A. (2018). Generation and Digital Correlation of Barker Code for Radars and Communication Systems. IJIREEICE, 6 (9), 1–6. https://doi.org/10.17148/ijireeice.2018.691
12. Tsmots, I. G., Riznyk, O. Ya., Balych, B. I., Lvovskij, Ch. Z. (2021). The method and simulation model for the synthesis of barker-like code sequences. Ukrainian Journal of Information Technology, 3 (2), 45–50. https://doi.org/10.23939/ujit2021.02.045
13. Siebert, W. M. (1988). The early history of pulse compression radar-the development of AN/FPS-17 coded-pulse radar at Lincoln Laboratory. IEEE Transactions on Aerospace and Electronic Systems, 24 (6), 833–837. https://doi.org/10.1109/7.18655
14. Blunt, S. D., Mokole, E. L. (2016). Overview of radar waveform diversity. IEEE Aerospace and Electronic Systems Magazine, 31 (11), 2–42. https://doi.org/10.1109/maes.2016.160071
15. Zhang, Y.-X., Liu, Q.-F., Hong, R.-J., Pan, P.-P., Deng, Z.-M. (2016). A Novel Monopulse Angle Estimation Method for Wideband LFM Radars. Sensors, 16 (6), 817. https://doi.org/10.3390/s16060817
16. Seleym, A. (2016). Complementary phase coded LFM waveform for SAR. 2016 Integrated Communications Navigation and Surveillance (ICNS), 4C3-1-4C3-5. https://doi.org/10.1109/icnsurv.2016.7486346
17. Levanon, N., Cohen, I., Itkin, P. (2017). Complementary pair radar waveforms–evaluating and mitigating some drawbacks. IEEE Aerospace and Electronic Systems Magazine, 32 (3), 40–50. https://doi.org/10.1109/maes.2017.160113
18. Azouz, A., Abosekeen, A., Nassar, S., Hanafy, M. (2021). Design and Implementation of an Enhanced Matched Filter for Sidelobe Reduction of Pulsed Linear Frequency Modulation Radar. Sensors, 21 (11), 3835. https://doi.org/10.3390/s21113835
19. Liu, M., Li, Z., Liu, L. (2018). A Novel Sidelobe Reduction Algorithm Based on Two-Dimensional Sidelobe Correction Using D-SVA for Squint SAR Images. Sensors, 18 (3), 783. https://doi.org/10.3390/s18030783
20. Azouz, A. (2020). Novel Sidelobe cancellation for Compound-Barker Combined with LFM or Polyphase Waveform. 2020 12th International Conference on Electrical Engineering (ICEENG), 268–276. https://doi.org/10.1109/iceeng45378.2020.9171777
21. Saari, V. (2011). Continuous-time low-pass filters for integrated wideband radio receivers. Aalto University. Available at: https://core.ac.uk/download/pdf/80703915.pdf
22. Kiranmai, B., Rajesh Kumar, P. (2015). Performance Evaluation of Compound Barker Codes using Cascaded Mismatched Filter Technique. International Journal of Computer Applications, 121 (19), 31–34. https://doi.org/10.5120/21649-4844
23. El-Tokhy, M. A., Mansour, H. A. K. (2008). A 2.3-mW 16.7-MHZ Analog Matched Filter Circuit For DS-CDMA Wireless Applications. Progress In Electromagnetics Research B, 5, 253–264. https://doi.org/10.2528/pierb08022406
24. Haji Ali, S. M., Shaker, M. M., Salih, T. (2018). Design and implementation of a dynamic analog matched filter using FPAA technology. World Academy of Science, Engineering and Technology, 206–210. Available at: https://www.researchgate.net/publication/322683048_Design_and_Implementation_of_a_Dynamic_Analog_Matched_Filter_Using_FPAA_Technology
25. Lari, M. (2023). Matched-filter design to improve self-interference cancellation in full-duplex communication systems. Wireless Networks, 29 (7), 3137–3150. https://doi.org/10.1007/s11276-023-03352-2
26. Hahm, M. D., Friedman, E. G., Titlebaum, E. L. (1997). A comparison of analog and digital circuit implementations of low power matched filters for use in portable wireless communication terminals. IEEE Transactions on Circuits and Systems II: Analog and Digital Signal Processing, 44 (6), 498–506. https://doi.org/10.1109/82.592584
27. Angarita Malaver, E. F., Barrera Lombana, N., Moreno Rubio, J. J. (2024). Smith Chart-Based Design of High-Frequency Broadband Power Amplifiers. Electronics, 13 (20), 4096. https://doi.org/10.3390/electronics13204096
28. Chen, S., Sun, H., Weng, M., Wen, S., Li, L., Liu, B. (2023). Design and Research of Channel Circuit Based on Broadband Power Line Carrier. Journal of Physics: Conference Series, 2433 (1), 012017. https://doi.org/10.1088/1742-6596/2433/1/012017
29. Thakur, S., Singh, R., Sharma, S. (2015). Dynamic Capacity Scheduling in Hadoop. International Journal of Computer Applications, 125 (15), 25–28. https://doi.org/10.5120/ijca2015906178
30. Qian, N., Zhou, D., Shu, H., Zhang, M., Wang, X., Dai, D. et al. (2025). Analog parallel processor for broadband multifunctional integrated system based on silicon photonic platform. Light: Science & Applications, 14 (1). https://doi.org/10.1038/s41377-025-01753-w
31. Oluwajobi, F., Wasiu, L. (2014). Multisim Design and Simulation of 2.2GHz LNA for Wireless Communication. International Journal of VLSI Design & Communication Systems, 5 (4), 65–74. https://doi.org/10.5121/vlsic.2014.5405
32. Li, Z., Li, X., Jiang, D., Bao, X., He, Y. (2020). Application of Multisim Simulation Software in Teaching of Analog Electronic Technology. Journal of Physics: Conference Series, 1544 (1), 012063. https://doi.org/10.1088/1742-6596/1544/1/012063
33. Berkman, L. N., Varfolomeieva, O. H., Hrushevska, V. P. (2015). Typovi syhnaly ta zavady v elektrozviazku. Kyiv: DUT NNITI, 92.
34. Galli, S., Logvinov, O. (2008). Recent Developments in the Standardization of Power Line Communications within the IEEE. IEEE Communications Magazine, 46 (7), 64–71. https://doi.org/10.1109/mcom.2008.4557044
35. Ndjiongue, A. R., Ferreira, H. C. (2019). Power line communications (PLC) technology: More than 20 years of intense research. Transactions on Emerging Telecommunications Technologies, 30 (7). https://doi.org/10.1002/ett.3575
36. Ustun Ercan, S. (2024). Power line Communication: Revolutionizing data transfer over electrical distribution networks. Engineering Science and Technology, an International Journal, 52, 101680. https://doi.org/10.1016/j.jestch.2024.101680
37. Balashov, V. O., Vorobienko, P. P., Liakhovetskyi, L. M., Pediash, V. V. (2012). Systemy peredavannia shyrokosmuhovymy syhnalamy. Odesa: Vyd. tsentr ONAZ im. O.S. Popova, 336. Available at: https://duikt.edu.ua/uploads/l_412_70653078.pdf